SUPERSONIC QUADRUPOLE NOISE THEORY FOR HIGH-SPEED HELICOPTER ROTORS

F. Farassat and Kenneth S. Brentner
Senior Research Scientist Research Engineer
NASA Langley Research Center
Hampton, Virgina

Abstract

High-speed helicopter rotor impulsive noise prediction is an important current problem of aeroacoustics. The deterministic quadrupoles have been shown to contribute significantly to high-speed impulsive (HSI) noise of rotors, particularly when the phenomenon of delocalization occurs. At high rotor-tip speeds, some of the quadrupole sources lie outside the sonic circle and move at supersonic speed. Brentner has given a formulation suitable for efficient prediction of quadrupole noise inside the sonic circle. In this paper, we give a simple formulation based on the acoustic analogy that is valid for both subsonic and supersonic quadrupole noise prediction. Like the formulation of Brentner, the model is exact for an observer in the far field and in the rotor plane and is approximate elsewhere. We give the full analytic derivation of this formulation in the paper. We present the method of implementation on a computer for supersonic quadrupoles using marching cubes for constructing the influence surface (Σ surface) of an observer space-time variable $(\mathbf{x}, t)$. We then present several examples of noise prediction for both subsonic and supersonic quadrupoles. It is shown that in the case of transonic flow over rotor blades, the inclusion of the supersonic quadrupoles improves the prediction of the acoustic pressure signature. We show the equivalence of the new formulation to that of Brentner for subsonic quadrupoles. It is shown that the regions of high quadrupole source strength are primarily produced by the shock surface and the flow over the leading edge of the rotor. The primary role of the supersonic quadrupoles is to increase the width of a strong acoustic signal.

1 Introduction

The efficient prediction of the high-speed impulsive (HSI) noise of helicopter rotors is currently an important problem of aeroacoustics. The cause of this noise has been identified since the late 1970's[1,2] as the deterministic quadrupoles in the vicinity of the rotor, and, in the case of delocalization, beyond the sonic circle and the blade tip. Many schemes have been proposed by researchers based on the acoustic analogy[3–9] and the Kirchhoff method.[10,11] At present, most of these schemes are limited to subsonic quadrupole source motion—supersonic quadrupole noise prediction appears to require further work to improve efficiency and robustness. In the case of subsonic quadrupole noise prediction, a method based on a formulation by Brentner, formulation Q1A, exists[7] which is exact for an in-plane, far-field observer but is approximate elsewhere. This method has been implemented in the code WOPWOP+[6,7] and has been shown to be highly efficient and robust. There is a need for an efficient and robust method of prediction of the supersonic quadrupole noise. We present a new formulation—based on the same model used by Brentner—that is valid for both subsonic and supersonic quadrupole noise prediction.

We give the derivation of the main result of this paper, formulation Q2, in Section 2. We start with an exact solution of the wave equation for quadrupole sources of the Ffowcs Williams–Hawkings (FW–H) equation given by Farassat and Brentner.[12] In this solution, volume integrals involving the quadrupole sources are only differentiated with respect to observer time. We write these volume integrals in terms of a surface integral over the collapsing sphere and a source time integral. For an observer in the rotor plane and in the far field, the collapsing sphere is approximated as a right cylinder normal to the rotor disc and the quadrupole source strength is integrated along lines normal to the rotor disc and treated as sources on the rotor disc. We then hypothesize that the quadrupole noise everywhere can be predicted using these surface sources. This hypothesis has been validated by Brentner and Holland.[6] The idea of approximating the volume (quadrupole) sources with equivalent surface sources was originally proposed and numerically implemented by Schmitz et al.[1] for the far-field solution of the FW–H equation. Later this idea was also implemented by Schultz and Splettstoesser,[3] Brentner and Holland,[6] and Brentner.[7] Our main contribution has been to use this idea in obtaining closed-form so-

Presented at the American Helicopter Society Technical Specialists' Meeting for Rotorcraft Acoustics and Aerodynamics, Williamsburg, Virginia, October 28 - 30, 1997.

lutions of the same equation, formulations Q1A and Q2, which seem to result in more efficient prediction of HSI noise. The new formulation presented here is very simple and is valid for both subsonic and supersonic quadrupoles. This gives us the opportunity to compare noise predictions from formulations Q1A and Q2 for subsonic quadrupoles.

In Section 3 we discuss how formulation Q2 is implemented in a new testbed code called WOPWOP2+. The quadrupole sources beyond the sonic circle can have multiple emission times and the usual solution of the wave equation for subsonic surface sources (e.g., formulations 1, 1A, and Q1A) will have a singularity known as the Doppler singularity. To avoid this Doppler singularity, it is necessary to use a Σ-surface formulation.[13,14] The method of construction of the Σ surface used in WOPWOP2+ is known as marching cubes[15]—an algorithm originally developed for computer graphics.[16]

Some examples of HSI noise prediction for a hovering rotor is presented in Section 4. First we present a comparison of the results of noise prediction for subsonic quadrupoles based on formulations Q1A and Q2. It is shown that the results agree well with each other. A study of the surface source strength (i.e., the integral of quadrupole source strength along the line normal to rotor disc) shows that the primary contributions to the quadrupole noise come from the shock surfaces on and beyond the blade and the flow over the leading edge of the blade. It is also shown that the inclusion of the quadrupole sources beyond the sonic circle improves the prediction of the width of the main pulse and the shape of the acoustic pressure signature and agreement with experimental data. Finally, we demonstrate the robustness of the formulation by performing predictions for out-of-plane and near-field observers. Concluding remarks follow in Section 5.

2 Formulation and Solution of the Problem

We begin with the solution of the following wave equation for quadrupole noise radiation from the Ffowcs Williams–Hawkings equation:

$$\Box^2 p'_Q(\mathbf{x},t) = \frac{\bar{\partial}^2}{\partial x_i \partial x_j}[T_{ij}H(f)] \qquad (1)$$

where T_{ij} is the Lighthill stress tensor, $H(f)$ is the Heaviside function, and $f=0$ describes the blade surface ($f>0$ outside the blade). The solution for this equation was given by Farassat and Brentner[12] as follows:

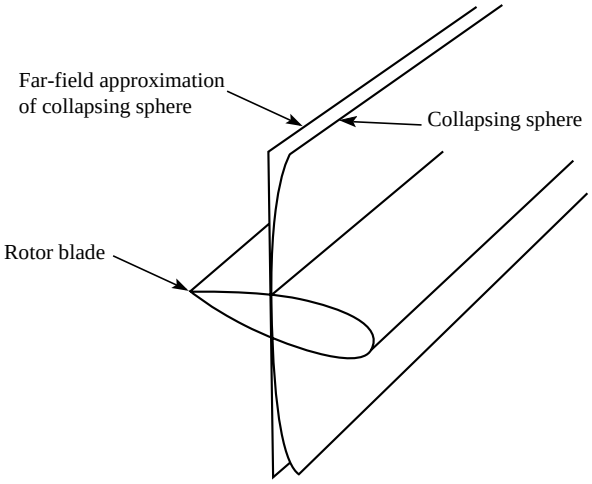

Figure 1. The actual and approximate collapsing sphere surfaces in the vicinity of the rotor blade.

$$\begin{aligned} 4\pi p'_Q(\mathbf{x},t) &= \frac{1}{c}\frac{\partial^2}{\partial t^2}\int_{-\infty}^{t}\int_{f>0}\frac{T_{rr}}{r}\,d\Omega\,d\tau \\ &+ \frac{\partial}{\partial t}\int_{-\infty}^{t}\int_{f>0}\frac{3T_{rr}-T_{ii}}{r^2}\,d\Omega\,d\tau \qquad (2) \\ &+ c\int_{-\infty}^{t}\int_{f>0}\frac{3T_{rr}-T_{ii}}{r^3}\,d\Omega\,d\tau \end{aligned}$$

where the quantity T_{rr} is the double contraction $T_{ij}\hat{r}_i\hat{r}_j$, and $\hat{r}_i$ are the components of the unit vector in the radiation direction. In addition, $d\Omega$ is an element of the collapsing sphere surface $g=0$. We now assume that the observer is in the far field and on the rotor plane. The part of the collapsing sphere intersecting the source region near the rotor blade can be approximated by a right cylinder normal to the rotor plane. This is shown in figure 1.

Let us assume that the rotor is nominally in the y_1y_2–plane and y_3 is, therefore, perpendicular to this plane (i.e., the rotor tip-path plane). We integrate the inner integrals of equation (2) with respect to y_3 over the approximate collapsing sphere surface. Let us define

$$Q_{ij}(y_1,y_2,\tau) = \int_{-\infty}^{\infty} T_{ij}\,dy_3 \qquad (3)$$

and use the relation

$$d\Sigma = c\,d\tau d, \qquad (4)$$

where d, is the length of an element of the curve defined by the intersection of the collapsing sphere with the rotor disc. Equation (2) can now be written as

$$\begin{aligned} 4\pi p'_Q(\mathbf{x},t) &= \frac{1}{c^2}\frac{\partial^2}{\partial t^2}\int \frac{1}{r}[Q_{rr}]_{ret}\, d\Sigma \\ &+ \frac{1}{c}\frac{\partial}{\partial t}\int \frac{1}{r^2}[3Q_{rr}-Q_{ii}]_{ret}\, d\Sigma \quad (5) \\ &+ \int \frac{1}{r^3}[3Q_{rr}-Q_{ii}]_{ret}\, d\Sigma\ . \end{aligned}$$

The integrals in equation (5) are all over the entire y_1y_2–plane. This allows us to bring the observer-time derivatives inside the integrals without worrying about the limits of integration.

The next step is the most crucial in the derivation of the final result. We note that $\partial/\partial t = \partial/\partial t|_{\mathbf{x}}$ meaning $\mathbf{x}$ in the frame fixed to the *undisturbed medium* is kept fixed in this differentiation. It must be understood that all velocity terms in $Q_{ij}(\mathbf{x},t)$ are specified with respect to the frame fixed to the undisturbed medium. However, if we use a change of coordinates $(\mathbf{x},t) \rightarrow (\boldsymbol{\eta},\tau)$, where the $\boldsymbol{\eta}$-frame is fixed to the rotor blade, we have

$$\begin{aligned} \frac{\partial [Q_{ij}]_{ret}}{\partial t}\Big|_{\mathbf{x}} &= \Big[\frac{\partial Q_{ij}}{\partial \tau}\Big|_{\boldsymbol{\eta}} - \mathbf{V}\cdot\nabla_{\boldsymbol{\eta}} Q_{ij}\Big]_{ret} \quad (6) \\ &\equiv L_\tau Q_{ij} \end{aligned}$$

where $\boldsymbol{\eta}$ is the position vector in the rotating frame and τ is the source time. Here $\mathbf{V} = \partial\boldsymbol{\eta}/\partial\tau$ is the velocity of the point with position vector $\boldsymbol{\eta}$ specified in the frame fixed to the undisturbed medium. We note that $\mathbf{V}$ is in the rotor plane. It is important to recognize that $Q_{ij}(\boldsymbol{\eta},\tau)$ actually stands for $Q_{ij}[\mathbf{x}(\boldsymbol{\eta},\tau),t(\tau)]$, where $t(\tau)=\tau$. Notice that the operator L_τ operates on Q_{ij} only. Using this operator notation in equation (5), we get

$$\begin{aligned} 4\pi p'_Q(\mathbf{x},t) &= \frac{1}{c^2}\int \frac{1}{r}\hat{r}_i\hat{r}_j L_\tau^2 Q_{ij}\, d\Sigma \\ &+ \frac{1}{c}\int \frac{1}{r^2}[3\hat{r}_i\hat{r}_j L_\tau Q_{ij} - L_\tau Q_{ii}]\, d\Sigma \\ &+ \int \frac{1}{r^3}[3Q_{rr}-Q_{ii}]_{ret}\, d\Sigma\ . \quad (7) \end{aligned}$$

To write this equation in final form we express $\mathbf{V}(\boldsymbol{\eta},\tau)$ as follows:

$$\mathbf{V} = \mathbf{V}_F + \omega\times\boldsymbol{\eta} \quad (8)$$

where $\mathbf{V}_F$ is the forward velocity of the rotor and $\boldsymbol{\eta}$ is the position vector of the source Q_{ij} in the rotor plane with the origin at the rotor center. We assume that both $\mathbf{V}_F$ and ω, the angular velocity vector of the rotor, are time independent. From equation (8), we have

$$\begin{aligned} \frac{\partial \mathbf{V}}{\partial\tau}\Big|_{\boldsymbol{\eta}} &= \omega\times(\omega\times\boldsymbol{\eta}) \\ &= -\omega^2\boldsymbol{\eta}\ . \quad (9) \end{aligned}$$

Thus, we can express L_τ^2 as follows:

$$\begin{aligned} L_\tau^2 &= (\frac{\partial}{\partial\tau}\Big|_{\boldsymbol{\eta}} - \mathbf{V}\cdot\nabla)(\frac{\partial}{\partial\tau}\Big|_{\boldsymbol{\eta}} - \mathbf{V}\cdot\nabla) \\ &= \frac{\partial^2}{\partial\tau^2}\Big|_{\boldsymbol{\eta}} - \mathbf{V}\cdot\nabla\frac{\partial}{\partial\tau}\Big|_{\boldsymbol{\eta}} - \frac{\partial}{\partial\tau}\Big|_{\boldsymbol{\eta}}(\mathbf{V}\cdot\nabla) \\ &\quad + \mathbf{V}\cdot\nabla(\mathbf{V}\cdot\nabla) \quad (10) \end{aligned}$$

All the gradients are with respect to $\boldsymbol{\eta}$. We have

$$\frac{\partial}{\partial\tau}(\mathbf{V}\cdot\nabla) = -\omega^2\eta\frac{\partial}{\partial\eta} + \mathbf{V}\cdot\nabla\frac{\partial}{\partial\tau} \quad (11)$$

where $\partial/\partial\eta$ is the directional derivative in the $\boldsymbol{\eta}$ (radial direction) and $\eta = |\boldsymbol{\eta}|$. We also have

$$\begin{aligned} \mathbf{V}\cdot\nabla(\mathbf{V}\cdot\nabla) &= (\omega\times\mathbf{V})\cdot\nabla + (\mathbf{V}\cdot\nabla')^2 \\ &= (\omega\times\mathbf{V}_F)\cdot\nabla - \omega^2\eta\frac{\partial}{\partial\eta} \\ &\quad + (\mathbf{V}\cdot\nabla')^2 \quad (12) \end{aligned}$$

where ∇' does not operate on $\mathbf{V}$, i.e.,

$$(\mathbf{V}\cdot\nabla')^2 = V_1^2\frac{\partial^2}{\partial\eta_1^2} + 2V_1V_2\frac{\partial^2}{\partial\eta_1\partial\eta_2} + V_2^2\frac{\partial^2}{\partial\eta_2^2} \quad (13)$$

and $\mathbf{V} = (V_1, V_2)$. Therefore, L_τ^2 can be written as

$$\begin{aligned} L_\tau^2 &= \frac{\partial^2}{\partial\tau^2}\Big|_{\boldsymbol{\eta}} - 2\mathbf{V}\cdot\nabla\frac{\partial}{\partial\tau}\Big|_{\boldsymbol{\eta}} + (\mathbf{V}\cdot\nabla')^2 \\ &\quad + (\omega\times\mathbf{V}_F)\cdot\nabla \quad (14) \end{aligned}$$

When this expression is used in equation (7), we get a singularity free expression for supersonic quadrupole noise prediction. We note that equation (7) has second space and time derivatives of Q_{ij} as well as first space derivatives in the $\eta_1\eta_2$–plane (the rotor plane). These quantities are available in the CFD postprocessor that is used to compute Q_{ij} for acoustic calculations. We will refer to equation (7) as formulation Q2. As it stands, formulation Q2 is valid for subsonic and supersonic quadrupole noise prediction for helicopter rotors in hover or forward flight. Note that this equation is very simple and has no singularities. We have assumed that the shocks on the blades are smeared over one or more grid cells and that Q_{ij} has continuous second derivatives over the rotor plane (although the magnitude of the second derivative can be very high at the foot of the shocks). These assumptions are

generally satisfied in CFD calculations for helicopter rotor aerodynamics.

2.1 Analysis of the Main Result

We will now do an order of magnitude study of the far-field term of our main result, equation (7). We can draw very useful conclusions from such a study as will be shown below. We know that the peak of directivity of quadrupole noise is in the rotor plane with the observer ahead of the helicopter. Let us put the observer in such a location in the far field. Then in the frame fixed to the undisturbed medium (where x_1-axis is the flight direction and the x_3-axis is normal to the rotor plane), the components of the unit radiation vector can be approximated as $\hat{\mathbf{r}} = (1, 0, 0)$. The major contribution to the far-field quadrupole noise comes from Q_{11} which we will look at closely below.

The numerator of the integrand of the far-field term is

$$L_\tau^2 Q_{11} = \frac{\partial^2 Q_{11}}{\partial \tau^2}\Big|_{\boldsymbol{\eta}} - 2\mathbf{V}\cdot\nabla\frac{\partial Q_{11}}{\partial \tau}\Big|_{\boldsymbol{\eta}} + (\mathbf{V}\cdot\nabla')^2 Q_{11} + (\omega \times \mathbf{V}_F)\cdot\nabla Q_{11} \tag{15}$$

We can now estimate the order of magnitude of each term in equation (15) as follows. Let the advancing tip speed be denoted by V_{AT} and $\omega = |\omega|$. Then, we see that

$$\frac{\partial^2 Q_{11}}{\partial \tau^2}\Big|_{\boldsymbol{\eta}} \sim \omega^2 Q_{11} \tag{16a}$$

$$\mathbf{V}\cdot\nabla\frac{\partial Q_{11}}{\partial \tau}\Big|_{\boldsymbol{\eta}} \sim \omega V_{AT}\frac{\partial Q_{11}}{\partial \eta_1} \tag{16b}$$

$$(\mathbf{V}\cdot\nabla')^2 Q_{11} \sim V_{AT}^2\frac{\partial^2 Q_{11}}{\partial \eta_1^2} \tag{16c}$$

$$(\omega \times \mathbf{V}_F)\cdot\nabla Q_{11} \sim \omega V_F\frac{\partial Q_{11}}{\partial \eta_1} \tag{16d}$$

In these equations, the derivative $\partial/\partial\eta_1$ is the directional derivative in the chordwise direction. Note that for a hovering rotor $\partial Q_{11}/\partial\tau$, $\partial^2 Q_{11}/\partial\tau^2$, and V_F are all zero, therefore the only remaining component is $(\mathbf{V}\cdot\nabla')^2 Q_{11}$. Since ω, in general, is small for helicopter rotors, we can see that the dominant term in forward flight is also most likely the term $(\mathbf{V}\cdot\nabla')^2 Q_{11}$. The right side of equation (16c) can be further estimated as

$$V_{AT}^2\frac{\partial^2 Q_{11}}{\partial \eta_1^2} \sim \frac{V_{AT}^2 Q_{11}}{(\Delta\eta_1)^2} \tag{17}$$

where $\Delta\eta_1$ is the chordwise scale over which significant change in Q_{11} occurs. This leads us to suspect that the dominant sources of quadrupole noise will be located along the leading edge of the rotor blade ($\Delta\eta_1 \sim LE$ radius) and along the shock trace in the rotor plane on and beyond the rotor tip ($\Delta\eta_1 \sim$ width of the projection of the shock surface in the rotor plane). These conclusions are verified by the computation of $L_\tau^2 Q_{11}$ for a hovering UH-1H model rotor blade at tip Mach number 0.925 shown in figure 2. It is apparent in the figure that the primary source of HSI noise is the shock wave (as proposed by Farassat and his colleagues—see references 12,17–19) and the flow over the leading edge of the blade. The significance of the quadrupole source in the leading edge region has not been widely recognized in previous work.

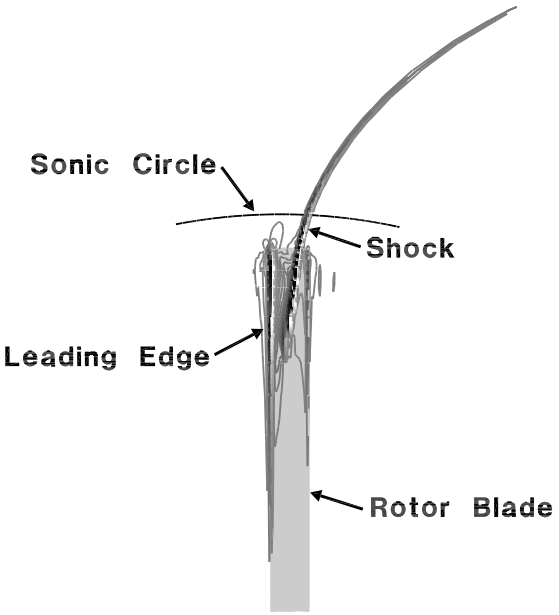

Figure 2. Contours of $L_\tau^2 Q_{11}$ in the vicinity of a hovering UH-1H rotor, $M_H = 0.925$.

3 Numerical Implementation

A new code, called WOPWOP2+, is used to demonstrate the utility of formulation Q2. WOPWOP2+ differs significantly from WOPWOP+[6,7] in that it uses a Σ-surface formulation to compute thickness and loading noise, as well as the quadrupole noise. The construction of the Σ surface and subsequent integration over the Σ surface is performed using the method of marching cubes integration developed by Brentner.[15] The numerical calculation of quadrupole noise has been divided into two stages: a preprocessing stage in which the integration of the Lighthill stress tensor in the normal direction, indicated in equation (3), is carried out, and an evaluation stage in which the quadrupole contribution to the acoustic pressure specified in equation (7) is determined. Both the preprocessor and the acoustic calculation are described briefly

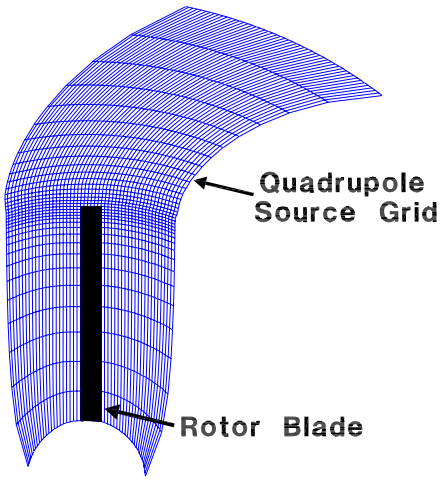

Figure 3. Typical quadrupole grid used for WOPWOP2+ calculations for hovering UH-1H rotor. Note that only every 4th grid line is shown in the chordwise direction.

in this section. More information on the preprocessor, which is the same preprocessor that is used by WOPWOP+, can be found in reference 6.

3.1 Preprocessor

Although the evaluation of Q_{ij} can be performed independently of observer position and retarded time, the preprocessor must read in the CFD solution, interpolate the solution at the necessary quadrature locations, and then perform the numerical quadrature in the direction normal to the rotor disc. The preprocessor needs knowledge of both the CFD grid topology and the solution format. In the implementation used for this work, the interpolation of the CFD data is two dimensional and is done one radial station at a time. For a given radial station, data are interpolated to quadrature points needed for composite Gauss-Legendre integration, on lines normal to the rotor plane. The lines are uniformly distributed in the chordwise direction. A two-dimensional linear least-squares interpolation is used to interpolate the density, momentum, and energy at each quadrature point. The Lighthill stress tensor T_{ij} is evaluated with the interpolated data. The value of Q_{ij} on the rotor disc is determined at each chordwise location before moving to the next radial station. The results are stored for the acoustic calculation stage. A typical grid generated by the quadrupole preprocessor is shown in figure 3.

3.2 WOPWOP2+

The primary function of the WOPWOP2+ code is to perform the integration indicated in equation (7) numerically. Although the integration is over the entire rotor disc plane, in practice the source strength is zero over a large part of the plane; hence, the quadrupole integration is only performed near the rotor blade (see figure 3). The main difficulty in the numerical evaluation of equation (7) is the construction of the Σ surface. The Σ surface is the collection of points in space-time that emit signals that reach the observer at one particular observer time. The integration is complex because the pointwise mapping between the physical source plane and the Σ surface is not known explicitly. Special care must be taken in the construction because in practice the Σ surface may be composed of several disjoint pieces when the source motion is supersonic—exactly the case we are interested in.

The marching cubes method begins constructing the Σ surface by choosing the source time and computing the corresponding observer time and integrand value at each grid point. If the observer times are computed and stored for each desired source time, the discrete computational data become a three-dimensional array; two computational indices parameterize the surface spatially and a third index accounts for the source time. In this three-dimensional computational space, isosurfaces of observer time t are, by definition, distinct realizations of the Σ surface. The extension of the marching-cubes algorithm for surface integration[15] determines how the surface intersects a logical cube in the three-dimensional computational grid, computes the contribution to the integral from that portion of the surface, and then moves (or marches) to the next cube. The topology of the surface within a single cube can be determined uniquely by examining the function value (observer time in this case) at each of the cube vertices and comparing this value to the desired surface value. A table lookup is then used to determine the exact topology of the surface in the current cube. The surface is formed by a set of triangular panels that have vertices on the edges of the cubes. The value of the surface integral over each triangle is approximated as the average integrand value of the triangle vertices multiplied by the triangle area. Linear interpolation is used to determine the integrand values at the triangle vertices based on the previously computed value at the cube vertices. The marching cubes algorithm is generic—the only difference in computing thickness, loading, or quadrupole noise is the value of the integrand computed at each grid vertex. (For more detail on the marching cubes algorithm, see references 15 and 16.)

For simplicity, the current WOPWOP2+ code only

implements formulation Q2 for a hovering rotor. For a hovering rotor, $L_\tau Q_{ij}$ and $L_\tau^2 Q_{ij}$ can be written in the simplified form

$$L_\tau Q_{ij} = \omega\eta \frac{\partial Q_{ij}}{\partial \eta_1} \tag{18a}$$

and

$$L_\tau^2 Q_{ij} = \omega^2\eta^2 \frac{\partial^2 Q_{ij}}{\partial \eta_1^2} \tag{18b}$$

where $\partial/\partial\eta_1$ is the directional derivative in the azimuthal direction and $\eta = |\boldsymbol{\eta}|$. Equation (18) is implemented numerically in WOPWOP2+ with a second-order accurate central-difference operators.

4 Numerical Results

In this section we first make a comparison of the acoustic pressure signatures of a hovering model rotor from WOPWOP+ and WOPWOP2+ which use formulations Q1A and Q2, respectively. Then, we present the comparison of the predicted and measured acoustic pressure signatures for the same hovering model rotor at four different tip Mach numbers. At the three highest tip Mach numbers, the phenomenon of delocalization occurs and WOPWOP2+ must be used for HSI noise prediction if the contribution of the supersonic quadrupoles is to be included in the prediction. The remaining analysis examines the role of the supersonic quadrupoles and the robustness of the formulation.

A model-scale rotor test conducted by Boxwell et al. in 1978[20] and repeated later by Purcell in 1988[21] is used for comparison. The measured data was for non-lifting hovering rotor generating HSI noise. The rotor was a 1/7th scale UH-1H main rotor with straight untwisted blades and NACA 0012 airfoil section. The rotor radius R was 1.045 m with a chord of 7.62 cm. The measured data reported here are all from a microphone in the rotor plane and at $3.09R$ from the rotor tip. The Euler solutions utilized as input in this numerical work were provided by Baeder and are described in references 5 and 22. The Euler solutions are also used for direct comparison with the acoustic prediction when experimental data is unavailable.

4.1 Comparison of Formulations

Figure 4 shows a comparison of the predicted acoustic pressure signatures from WOPWOP+ (formulation Q1A) and WOPWOP2+ (formulation Q2) at tip Mach number 0.925. The thickness and loading, quadrupole, and total acoustic pressure time histories predicted by each of the codes are also shown in this figure. Although the supersonic quadrupoles are important in prediction of the acoustic pressure signature because delocalization occurs at this operating condition, WOPWOP+ can only handle subsonic quadrupole sources; therefore, we have only used the subsonic quadrupole sources in both predictions for this comparison. We have utilized the marching cubes approach to construct the Σ surface (influence surface) of the rotor blade and the quadrupole source surface in WOPWOP2+. A good agreement in this comparison proves two points. First, it will tell us that the construction of the Σ surface is correct in WOPWOP2+. Second, the two formulations Q1A and Q2 are equivalent. Both these points are evident in figure 4. This figure also shows that the individual components due to thickness and loading and the quadrupole sources as well as the total acoustic pressure signatures from the two codes agree well. Thus, we have established some confidence in using WOPWOP2+ for prediction of HSI noise.

4.2 Comparison with Measured Data

We now present HSI noise calculations for tip Mach numbers 0.88, 0.9, 0.925, and 0.95 in figure 5. The quadrupole grid extends $0.788R$ beyond the blade tip for all the WOPWOP2+ calculations shown in figure 5. For comparison, we have also shown the WOPWOP+ signature which includes quadrupole sources up to the sonic circle. It is seen that the agreement of the WOPWOP2+ signature with the measured data is excellent and better than that of WOPWOP+ for each case. For the more intense cases, $M_H = 0.925$ and 0.95, the agreement of the WOPWOP+ prediction with the measured acoustic pressure signature is not fully satisfactory. The acoustic pressure signature from WOPWOP2+, however, agrees well with the measured signature even in the value of the negative peak. We have, thus, demonstrated, the ability to predict the noise from supersonic quadrupoles in the case of delocalized shocks and the resulting improvements in the overall shape and level of the acoustic pressure.

We point out that the WOPWOP2+ predictions have oscillations which appear to be numerical in origin for the delocalized cases $M_H = 0.9$, 0.925, and 0.95. We have been unable to fully determine the cause of these oscillations, but we know that the oscillations come from the supersonic quadrupole sources somewhat beyond the sonic circle. Note in Figure 3 that the radial spacing of the quadrupole grid, which is based upon the radial spacing of the CFD grid, grows significantly beyond the tip of the rotor blade. We do not believe the oscillations in the acoustic signal are primarily a result of inaccuracies in the numerical computation of the derivatives specified in equation (18) because the largest gradients are located on the blade surface and are included in the subsonic quadrupole

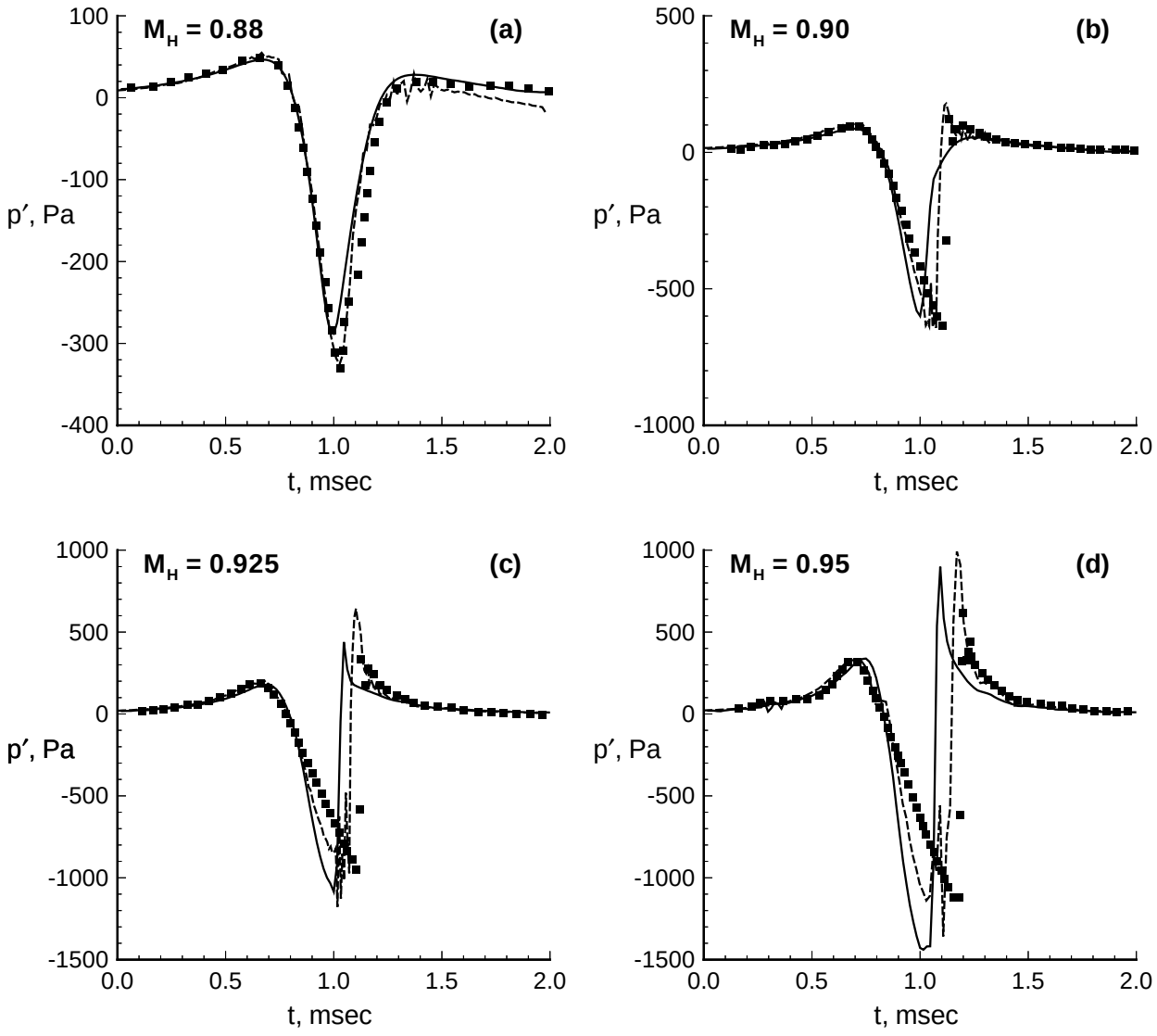

Figure 5. Comparison of WOPWOP+ (——) and WOPWOP2+ (– – –) predicted acoustic pressure with experimental data[21] (■) for hovering model UH-1H rotor. Quadrupole grid in WOPWOP+ prediction extended almost to sonic circle and in WOPWOP2+ predictions extended $0.788R$ beyond the rotor tip. (a) $M_H = 0.88$; (b) $M_H = 0.90$; (c) $M_H = 0.925$; (d) $M_H = 0.95$.

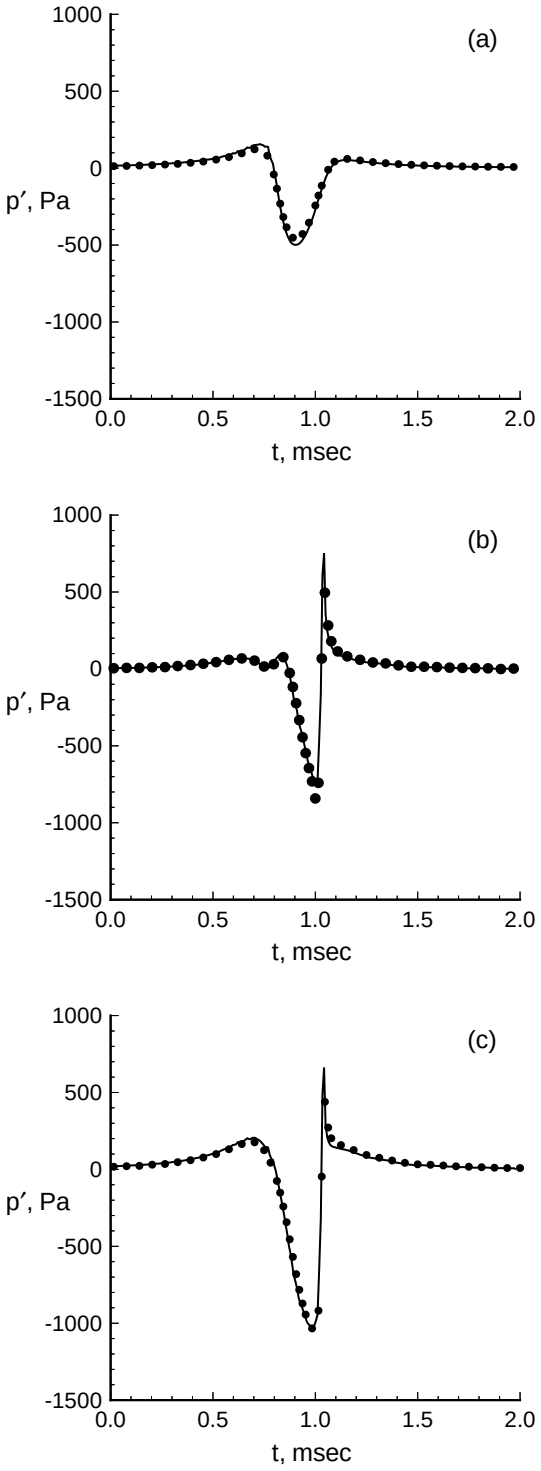

Figure 4. Comparison of WOPWOP+ prediction (•) with subsonic WOPWOP2+ prediction (——) for a UH-1H hovering rotor, $M_H = 0.925$. Quadrupole grid extends $0.075R$ beyond rotor tip. (a) thickness and loading components; (b) quadrupole component; (c) total acoustic pressure.

calculations. Further work is necessary to understand the source of the oscillations and how to eliminate them.

It is well known that the quadrupole accounts for the nonlinear propagation effects caused by the finite particle velocity and the variation of sound speed in the physical problem. The calculations shown in figure 5 seems to indicate that the primary role of the supersonic quadrupoles is to increase the pulse width of intense propagating waves. The width of the main pulse of the signatures predicted by WOPWOP2+ is only slightly narrower than the measured signature. Even for the $M_H = 0.88$ case, which is not delocalized, the supersonic quadrupoles improve the agreement by increasing the width and amplitude of the acoustic signal. For the delocalized cases, the supersonic quadrupoles also decrease the slope, and thus improve the agreement, of the triangular shape proceeding the rapid shock-like increase in acoustic pressure. Figure 6 shows the effect of the extent of the quadrupole grid for the particularly intense $M_H = 0.95$ case. Three separate computations were made with the quadrupole source grid extending beyond the rotor tip $0.05R$, $0.79R$, and $1.86R$, respectively. The quadrupole grid is shown in figure 6a with the three grid extents indicated. The first WOPWOP2+ computation, $0.05R$ beyond the rotor tip, is essentially identical to the WOPWOP+ calculation shown in figure 5d. Notice that the prediction for the largest grid extent, $1.86R$ beyond the rotor tip, agrees very well with the data in both waveform amplitude, width, and shape. (We suspect that the oscillations in the signal after the waveform are related to the extremely coarse radial resolution of the grid between $r/R = 1.79$ and $r/R = 2.86$.) These computations suggest two things: even though the quadrupole correctly predicts the nonlinear propagation (i.e., the widening and changing of the waveform shape), it is probably an inefficient tool for predicting the nonlinear propagation because an accurate CFD computation must proceed the quadrupole prediction; and it seems likely that the nonlinear propagation could be more appropriately by another, possibly one-dimensional method, starting with the acoustic signal somewhat closer to the rotor.

4.3 Formulation Robustness

In this section we wish to demonstrate the robustness of the method by performing predictions which violate some of the assumptions leading to formulation Q2. First we predict the noise for out-of-plane observer and compare the acoustic pressure with an Euler solution. Secondly, we predict the noise for a very near-field observer.

The acoustic pressure was predicted using WOP-

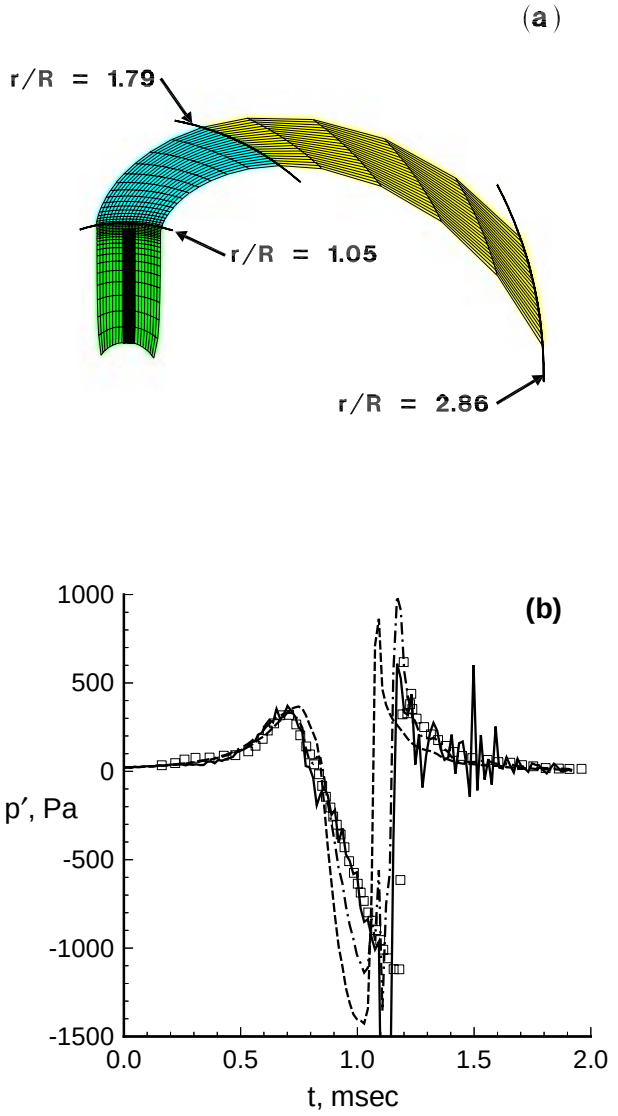

Figure 6. Effect of quadrupole grid extent shown for hovering UH-1H rotor, $M_H = 0.95$. (a) quadrupole grid (every 10th grid line in chordwise direction shown); (b) predicted acoustic pressure for three quadrupole grid extents: – – – , $0.05R$ beyond rotor tip (subsonic); –·–, $0.79R$ beyond rotor tip; ——, $1.86R$ beyond rotor tip; ▫ experimental data.[21]

WOP+ and WOPWOP2+ at two observer locations directly below the an in-plane observer at $3.09R$ from the rotor hub. These observers are 10 and 20 deg below the rotor plane, respectively. In figure 7 we show these prediction for the $M_H = 0.9$ case. No measured data are available at these observer locations, therefore, we have interpolated the Euler solutions[5] used as input. It is seen that the two sets of calculations agree well with each other, but the WOPWOP2+ result is slightly better for the 10 deg down observer. Furthermore, as expected, the peak negative value of the main pulse of the acoustic pressure reduces with increasing observer angle. The quadrupole contribution below 20 deg is very small.

In a second comparison, shown in figure 8, we have predicted the acoustic pressure with WOPWOP2+ at an in-plane observer $1.094R$ from the rotor hub. This observer is *inside* the sonic circle and is less than two chordlengths from the rotor tip at the closest distance. The quadrupole grid extends almost to the observer. WOPWOP+ was unable to determine the retarded time satisfactorily for this severe test case. The WOPWOP2+ prediction slightly underpredicts the Euler solution; nevertheless, the comparison is really extremely good at this very near-field location. In particular, the WOPWOP2+ prediction agrees perfectly with the Euler data both before the negative peak and for the curved part of the signal at the top of the shock-like structure after the negative peak. The far-field and near-field quadrupole terms (terms with $1/r$ dependence and terms with $1/r^2$ and $1/r^3$ dependence, respectively) from equation (7) are also shown in figure 8. Clearly the near-field quadrupole terms—usually neglected by other researchers—contribute significantly to the correct prediction of waveform shape at this close distance. Figure 8 demonstrates the importance of keeping all of the terms so that the acoustic prediction can be compared directly with CFD.[12] Both figures 7 and 8 demonstrate the robustness of formulation Q2.

5 Concluding Remarks

We have presented a new quadrupole noise prediction method based on a new analytic result, called formulation Q2, valid for both subsonic and supersonic quadrupole sources. The new formulation is very simple and without any singularity. The procedure for implementation of the result is discussed in the paper. This new code is called WOPWOP2+. We have demonstrated that formulation Q2 is equivalent to formulation Q1A of Brentner used in WOPWOP+ for subsonic quadrupole sources. By order of magnitude study of the formulation Q2 far-field integrand, we have shown that the shock surfaces and the stagna-

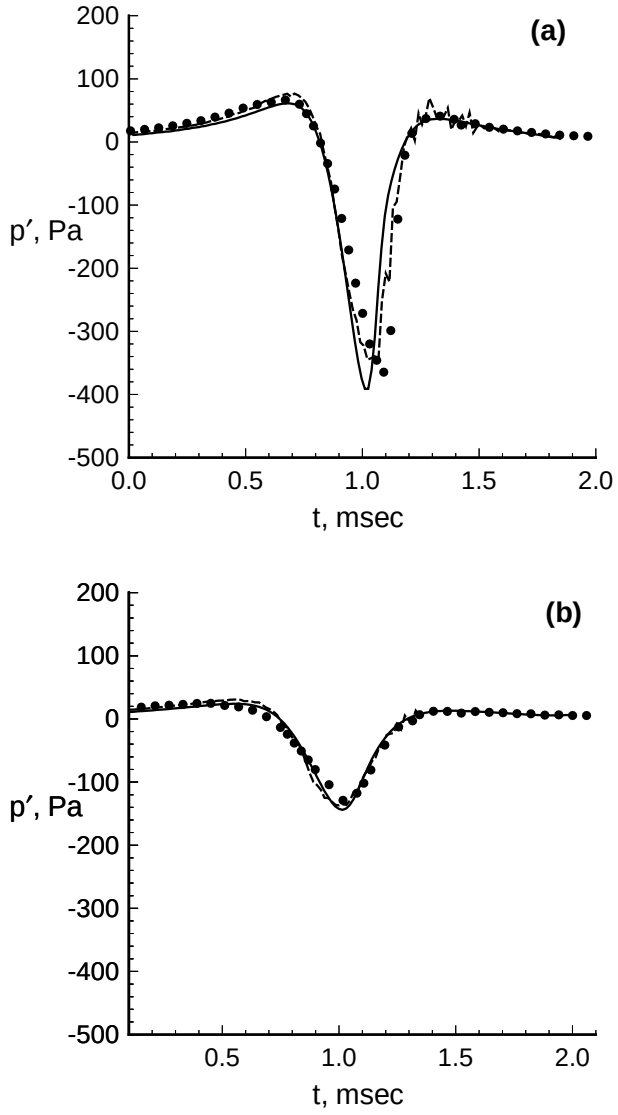

Figure 7. Comparison of WOPWOP+ (——), WOPWOP2+ (– – –), and Euler[5,22] (•) predicted acoustic pressures for hovering model UH-1H rotor, $M_H = 0.90$. (a) 10 deg below rotor plane; (b) 20 deg below rotor plane.

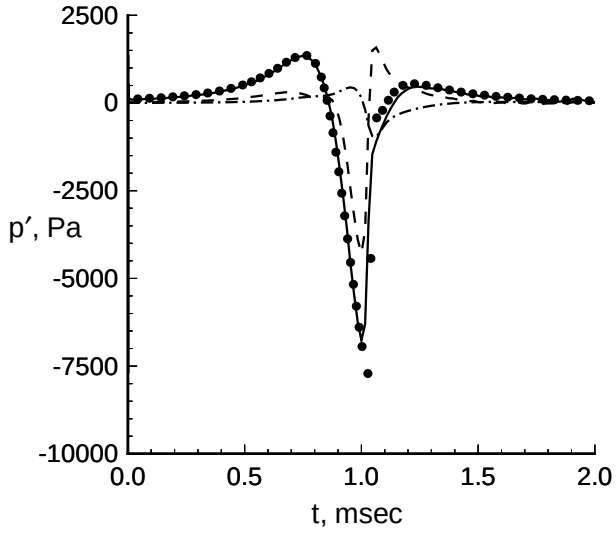

Figure 8. Near-field noise prediction at in-plane observer located $1.094R$ from rotor hub for hovering model UH-1H rotor, $M_H = 0.90$ with quadrupole grid $0.0935R$ beyond rotor tip. – – –, far-field quadrupole component; –·–, near-field quadrupole components; ——, WOPWOP2+ total acoustic pressure; •, Euler[5,22] total acoustic pressure.

tion flow at the leading edge of the blade are regions of high source intensity. We have shown that for rotors operating at high tip Mach numbers—before and after delocalization—the new formulation predicts acoustic pressure signatures which agree well with the experimental data in both the shape and the level of the main pulse of the signature. We have also shown that the supersonic quadrupoles widen and modify the shape of the waveform. A new and robust option is now available for prediction of HSI noise of helicopter rotors based on formulation Q2.

References

1. Yu, Y. H., Caradonna, F. X., and Schmitz, F. H., "The Influence of the Transonic Flow Field on High-Speed Helicopter Impulsive Noise," Fourth European Rotorcraft and Powered Lift Aircraft Forum, 1978. Paper 58.

2. Hanson, D. B., and Fink, M. R., "The Importance of Quadrupole Sources in Prediction of Transonic Tip Speed Propeller Noise," *Journal of Sound and Vibration*, Vol. 62, No. 1, 1979, pp. 19–38.

3. Schultz, K. J., and Splettstoesser, W. R., "Prediction of Helicopter Rotor Impulsive Noise Using

Measured Blade Pressure," American Helicopter Society 43rd Annual Forum, 1987.

4. Prieur, J., "Calculation of Transonic Rotor Noise Using a Frequency Domain Formulation," AIAA Paper 86-1901, 1986.

5. Baeder, J. D., "Euler Solutions to Nonlinear Acoustics of Non-Lifting Rotor Blades," American Helicopter Society/Royal Aeronautical Society International Technical Specialists' Meeting on Rotorcraft Acoustics and Rotor Fluid Dynamics, Oct. 1991.

6. Brentner, K. S., and Holland, P. C., "An Efficient and Robust Method for Computing Quadrupole Noise," *Journal of the American Helicopter Society*, Vol. 42, No. 2, Apr. 1997, pp. 172–181.

7. Brentner, K. S., "An Efficient and Robust Method for Predicting Helicopter Rotor High-Speed Impulsive Noise," *Journal of Sound and Vibration*, Vol. 203, No. 1, 1997.

8. di Francescantonio, P., "A New Boundary Integral Formulation for the Prediction of Sound Radiation," *Journal of Sound and Vibration*, Vol. 202, No. 4, 1997, pp. 491–509.

9. Brentner, K. S., and Farassat, F., "An Analytical Comparison of the Acoustic Analogy and Kirchhoff Forumulation for Moving Surfaces," American Helicopter Society 53rd Annual Forum, 1997.

10. Brentner, K. S., Lyrintzis, A. S., and Koutsavdis, E. K., "Comparison of Computational Aeroacoustic Prediction Methods for Transonic Rotor Noise Prediction," *Journal of Aircraft*, Vol. 34, No. 4, July-Aug. 1997, pp. 531–538.

11. Strawn, R. C., and Biswas, R., "Computation of Helicopter Rotor Noise in Forward Flight," *Journal of the American Helicopter Society*, Vol. 40, No. 3, July 1995, pp. 66–72.

12. Farassat, F., and Brentner, K. S., "The Uses and Abuses of the Acoustic Analogy in Helicopter Rotor Noise Prediction," *Journal of the American Helicopter Society*, Vol. 33, No. 1, Jan. 1988, pp. 29–36.

13. Farassat, F., "Theory of Noise Generation from Moving Bodies with an Application to Helicopter Rotors," NASA TR R-451, 1975.

14. Farassat, F., "Introduction to Generalized Functions With Applications in Aerodynamics and Aeroacoustics," NASA TP 3428, May 1994. See corrected version, April 1996.

15. Brentner, K. S., "A New Algorithm for Computing Acoustic Integrals," *Proceedings of the IMACS 14th World Congress on Computational and Applied Mathematics*, Vol. 2, 1994, pp. 592–595.

16. Lorensen, W. E., and Cline, H. E., "Marching Cubes: A High Resolution 3D Surface Construction Algorithm," *Computer Graphics*, Vol. 21, No. 4, July 1987, pp. 163–169.

17. Farassat, F., "Quadrupole Source in Prediction of Noise of Rotating Blades—A New Source Description," AIAA Paper 87-2675, 1987.

18. Farassat, F., Lee, Y.-J., Tadghighi, H., and Holz, R., "High-Speed Helicopter Rotor Noise—Shock Waves as a Potent Source of Sound," American Helicopter Society/Royal Aeronautical Society International Technical Specialists' Meeting on Rotorcraft Acoustics and Rotor Fluid Dynamics, Oct. 1991.

19. Tadghighi, H., Holz, R., Farassat, F., and Lee, Y. J., "Development of a Shock Noise Prediction Code for High-Speed Helicopters," American Helicopter Society 47th Annual Forum, 1991.

20. Boxwell, D. A., Yu, Y. H., and Schmitz, F. H., "Hovering Impulsive Noise: Some Measured and Calculated Results," *Vertica*, Vol. 3, No. 1, 1979, pp. 35–45. Also in NASA CP-2052, 1978.

21. Purcell, T. W., "CFD and Transonic Helicopter Sound," Fourteenth European Rotorcraft Forum, 1988. Paper 2.

22. Baeder, J. D., Gallman, J. M., and Yu, Y. H., "A Computational Study of Aeroacoustics of Rotors in Hover," *Journal of the American Helicopter Society*, Vol. 42, No. 1, Jan. 1997, pp. 39–53.